

This article was downloaded by:

On: 25 January 2011

Access details: *Access Details: Free Access*

Publisher *Taylor & Francis*

Informa Ltd Registered in England and Wales Registered Number: 1072954 Registered office: Mortimer House, 37-41 Mortimer Street, London W1T 3JH, UK



Liquid Crystals

Publication details, including instructions for authors and subscription information:

<http://www.informaworld.com/smpp/title~content=t713926090>

High birefringence and low viscosity negative dielectric anisotropy liquid crystals

Sebastian Gauza^a; Meizi Jiao^a; Shin-Tson Wu^a; Przemysław Kula^b; Roman Dąbrowski^b; Xiao Liang^c

^a College of Optics and Photonics, University of Central Florida, Orlando, FL 32816, USA ^b Institute of Chemistry, Military University of Technology, 00-908 Warsaw, Poland ^c Department of Chemistry, Tsinghua University, Beijing 100084, P.R. China

Online publication date: 06 July 2010

To cite this Article Gauza, Sebastian , Jiao, Meizi , Wu, Shin-Tson , Kula, Przemysław , Dąbrowski, Roman and Liang, Xiao(2008) 'High birefringence and low viscosity negative dielectric anisotropy liquid crystals', *Liquid Crystals*, 35: 12, 1401 – 1408

To link to this Article: DOI: 10.1080/02678290802624381

URL: <http://dx.doi.org/10.1080/02678290802624381>

PLEASE SCROLL DOWN FOR ARTICLE

Full terms and conditions of use: <http://www.informaworld.com/terms-and-conditions-of-access.pdf>

This article may be used for research, teaching and private study purposes. Any substantial or systematic reproduction, re-distribution, re-selling, loan or sub-licensing, systematic supply or distribution in any form to anyone is expressly forbidden.

The publisher does not give any warranty express or implied or make any representation that the contents will be complete or accurate or up to date. The accuracy of any instructions, formulae and drug doses should be independently verified with primary sources. The publisher shall not be liable for any loss, actions, claims, proceedings, demand or costs or damages whatsoever or howsoever caused arising directly or indirectly in connection with or arising out of the use of this material.

High birefringence and low viscosity negative dielectric anisotropy liquid crystals

Sebastian Gauza^{a*}, Meizi Jiao^a, Shin-Tson Wu^a, Przemysław Kula^b, Roman Dąbrowski^b and Xiao Liang^c

^aCollege of Optics and Photonics, University of Central Florida, Orlando, FL 32816, USA; ^bInstitute of Chemistry, Military University of Technology, 00-908 Warsaw, Poland; ^cDepartment of Chemistry, Tsinghua University, Beijing 100084, P. R. China

(Received 2 October 2008; final form 13 November 2008)

We have synthesised and evaluated the physical properties of some high birefringence, lateral difluoro-terphenyl compounds and mixtures. These mixtures exhibit a high birefringence ($\Delta n \sim 0.24$) in the visible spectral range and a relatively low viscosity. When doped in commercial mixtures, the difluoro-terphenyl compounds enhance the mixture's birefringence while causing almost no penalty to the rotational viscosity. These mixtures are particularly attractive for achieving fast response times in thin-cell liquid crystal displays.

Keywords: high birefringence; fluorinated terphenyl; liquid crystals; vertical alignment; response time

1. Introduction

Nematic liquid crystals (NLCs) with a negative dielectric anisotropy ($\Delta\epsilon < 0$) play an important role in many electro-optical devices. For example, a vertical alignment (VA) cell using a negative $\Delta\epsilon$ LC exhibits a high contrast ratio (I) which is particularly attractive for video applications. Besides a high contrast ratio, a fast response time is very desirable for almost all LC devices, especially for reducing the motion blur of liquid crystal display televisions (LCD TVs) and the colour break-up of colour sequential LCDs. For transmissive LCD TVs (2), a typical cell gap is $3.5\mu\text{m}$ and the trend is to go thinner. In colour-sequential projection displays using a single reflective liquid-crystal-on-silicon (LCoS) panel (3), colour break-up would be negligible if the LC response time could be reduced to $\sim 1\text{ms}$ (4). A typical cell gap for LCoS is $2\mu\text{m}$, in which colour break-up is still noticeable. Reducing cell gap is a straightforward approach to improving response time because the LC response time is proportional to the LC layer thickness (d) as $\tau_0 \sim d^x$, where the exponent x is dependent on the surface anchoring energy; it varies between 2 and 1 from strong to weak anchoring (5–8). A high birefringence LC material enables a thinner cell gap to be used while keeping the same phase retardation, i.e. $d\Delta n/\lambda$ (9–13).

The rise time and decay time of a VA cell are given as follows (5, 14):

$$\tau_{\text{rise}} \sim \tau_0 \left(\left(\frac{V}{V_{th}} \right)^2 - 1 \right), \quad (1)$$

$$\tau_{\text{decay}} \sim \tau_0 = \gamma_1 d^2 / K_{33} \pi^2, \quad (2)$$

where V is the turn-on voltage, V_{th} is the threshold voltage, γ_1 is the rotational viscosity, and K_{33} is the

bend elastic constant. Therefore, it is important not only to increase birefringence but also to maintain low visco-elastic coefficient (γ_1/K_{33}). Elongating the π -electron conjugation of the LC compounds is the most effective way to increase birefringence (9, 14–18). Common functional groups that contribute to the conjugation lengths include unsaturated rings, such as phenyl rings, and unsaturated bonds, such as carbon–carbon double (19–21) or triple bonds (22–24). Among unsaturated carbon–carbon bonds, stilbene (25, 26) and diacetylene (27, 28) are not stable under ultraviolet illumination and should be avoided.

Negative dielectric anisotropy ($\Delta\epsilon < 0$) can be achieved by introducing polar groups in the lateral positions of a LC compound. A widely adopted structure is the lateral (2,3) difluoro substitutions on the phenyl ring. As a result, the effective dipole moment is perpendicular to the principal molecular axis. Considering the photochemical stability of the liquid crystal molecules with a certain structure of a rigid core, we selected the terphenyl unit as a base system with elongated π -electron conjugation. Moreover, with three phenyl rings linked by a single carbon–carbon bond we could obtain multiple options for lateral (2,3) difluoro substitution. Four distinct examples shown in (29) are: 2,3,2',3',2'',3''-hexafluoro-4-butyl-4''-butyl-[1,1';4,4']terphenyl, 2,3,2'',3''-tetrafluoro-4-methyl-4''-butyl-[1,1';4,4']terphenyl, and 2',3',2'',3''-tetrafluoro-4-propyl-4''-pentyl-[1,1';4,4']terphenyl, and 2',3'-difluoro-4-ethyl-4''-pentyl-[1,1';4,4']terphenyl. Clearly, including more (2,3) difluorinated phenyl rings in the rigid core helps to increase the negative $\Delta\epsilon$ at the expense of increased viscosity and diminishing mesomorphism (29–33). Therefore,

*Corresponding author. Email: sgauza@mail.ucf.edu

taking high Δn , negative $\Delta\epsilon$, and low viscosity into consideration, the 2',3'-difluoro-4-alkyl-4''alkyl-[1,1';4',1'']-terphenyl structure is a promising candidate (29, 34). Some of the difluorinated negative $\Delta\epsilon$ compounds have been employed in many commercial LC mixtures for VA LCDs (29, 30).

In this paper, we report the physical properties and electro-optical performance of some recently synthesised 2',3'-difluoro-4-alkyl-4''alkyl-[1,1';4',1'']-terphenyl LC compounds and mixtures. Such a terphenyl-based mixture is used as dopant for commercial mixtures for enhancing their figure-of-merit (FoM). Potential applications of these mixtures for VA LCoS-based devices are addressed.

2. Experimental

Several techniques were used to characterise the physical properties of the single terphenyl compounds and mixtures. Differential scanning calorimetry (TA Instrument Model Q-100) was used to determine the phase transition temperatures. Results were obtained from 3 mg to 6 mg samples in the heating and cooling cycles at a scanning rate of 2°C min^{-1} .

To measure birefringence, we filled a $5\ \mu\text{m}$ homeotropic cell (pretilt angle $\sim 87^\circ$) and probed its phase retardation using a He-Ne laser ($\lambda = 633\ \text{nm}$) (35). At a given temperature, the phase retardation is related to cell gap d , birefringence Δn , and wavelength λ as:

$$\delta = 2\pi d\Delta n/\lambda. \quad (3)$$

In this study, we compared the compound performances based on the FoM which is defined as (36)

$$\text{FoM} = K_{33}\Delta n^2/\gamma_1, \quad (4)$$

where K_{33} is the bend elastic constant and γ_1 is the rotational viscosity. The temperature-dependent birefringence of an LC can be described as follows:

$$\Delta n = \Delta n_o S, \quad (5)$$

$$S = (1 - T/T_c)^\beta, \quad (6)$$

where Δn_o is the birefringence at $T=0\ \text{K}$, S is the order parameter, β is a material constant, and T_c is the clearing temperature of the LC. By fitting the experimental data using Equations (5) and (6), we can obtain Δn_o and β . Once these two parameters are determined, the LC birefringence at any temperature can be extrapolated.

Using Equation (4) and knowing that $K_{33} \sim S^2$ and $\gamma_1 \sim S \exp(E/kT)$, we can rewrite the FoM as follows (37):

$$\text{FoM} = a(\Delta n_o)^2 \left(1 - \frac{T}{T_c}\right)^{3\beta} \exp\left(\frac{-E}{\kappa T}\right), \quad (7)$$

where a is a proportionality constant. The FoM is commonly used to assess the performance of a LC compound or mixture because it is independent of the cell gap employed. The dielectric and elastic constants of the mixtures were measured by the capacitance method (37, 38) of a single homeotropic cell, using a computer-controlled LCAS II (LC-Vision) instrument.

3. Results and Discussion

Table 1 lists the molecular structures and phase transition temperatures of the laterally fluorinated terphenyl compounds we prepared. Compounds **1–5** have different length in the left and right alkyl terminal chains. Compound **1**, with a methyl terminal group, shows a fairly high melting temperature $T_M \sim 90.1^\circ\text{C}$. Replacing the methyl group with methoxy (compound **2**) does not change the T_M of the compound but increases its clearing temperature (T_c) by about 4°C . The heat fusion enthalpy of compounds **1** and **2** is almost the same (~ 6.1 to $6.2\ \text{kcal/mol}$) which is the highest among the homologues we investigated in this experiment. On the contrary, compounds **3** (ethyl-pentyl) and **4** (propyl-pentyl) have the lowest T_M at 44.7°C and 42.9°C , respectively, in the terphenyl series we studied. Moreover, their heat fusion enthalpy is about 30% lower than that of compounds **1** and **2**. Small heat fusion enthalpy is desirable for mixture formulation. The melting temperature gradually increases as the terminal alkyl chains of a compound become shorter (compounds **5–8**). As expected, compound **8**, with short and symmetric alkyl chains, exhibits the highest melting point. As shown in Table 1, the melting temperature of the terphenyl compounds strongly depends on the length of the two terminal alkyl chains. The more asymmetric compounds tend to have a lower melting temperature, except for the compound with a methyl group which is too short and too rigid to introduce good mesomorphic properties (see compound **1**). Based on mesomorphic properties, the most attractive compounds for mixture formulation among the presented structures are compounds **3** and **5**.

Therefore, after having evaluated the mesomorphic properties of single compounds, we formulated several

mixtures based on the compounds shown in Table 1. First, we formulated a eutectic terphenyl mixture consisting of compounds **1**, **3** and **4**. We designated this mixture as NLC-0100. We then mixed NLC-0100 to a commercial negative $\Delta\epsilon$ LC host (NLC-1000) at steps of 20 wt%. For simplicity, we named the experimental mixture containing 40 wt% host NLC-1000 and 60 wt% guest terphenyl NLC-0100 as NLC-4060, and so on. Afterwards, we measured their phase transition temperature, birefringence, visco-elastic coefficient and FoM.

Figure 1 shows the phase transition temperatures of the mixtures we prepared with a 20 wt% step increase of terphenyl mixture NLC-0100. The melting point of the host NLC-1000 is below -60°C . As the

concentration of terphenyl compound increases, the mixture's melting temperature increases substantially. From the phase transition diagram shown in Figure 1, the projected eutectic point seems to occur at 20% of NLC-0100; this means that the melting point of NLC-8020 should be lower than -60°C . For NLC-6040 (60 wt% host mixture+40 wt% terphenyl), the melting point occurs at -10°C during the heating cycle but the supercooling effect pushes the crystallisation point to below -50°C . As the terphenyl concentration increases to 60% (NLC-4060), the melting point increases to about 5°C . This is too high for practical applications from a storage viewpoint. Although failing the commercial standards for storage at low temperature, these three mixtures

Table 1. Mesomorphic properties of the eight laterally difluoro-terphenyl compounds studied.

No	Compound	T_m [$^\circ\text{C}$]	ΔH [kcal/mol]	T_c [$^\circ\text{C}$]
1		90.1	6.1	159.9
2		90.0	6.2	164.2
3		44.7	4.8	110.2
4		42.9	3.9	122.5
5		52.1	5.1	112.4
6		59.9	4.4	119.6
7		69.4	5.8	103.3
8		95.8	5.3	130.0

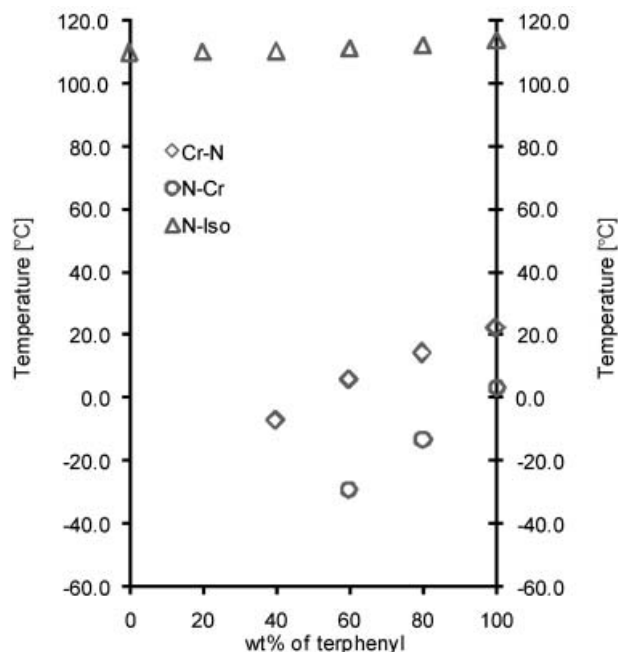


Figure 1. Phase transition temperatures for the NLC binary systems. Here, binary stands for the mixture between NLC-1000 and NLC-0100, a eutectic of three terphenyl compounds.

(NLC-4060, NLC-2080, and NLC-0100) are still valuable for evaluating the physical properties of terphenyl compounds at elevated temperatures.

We have measured the physical properties of these mixtures at elevated temperatures. To illustrate the results we chose isothermote binary diagrams which present birefringence, visco-elastic coefficient and FoM values, respectively, in Figures 2(a), 2(b) and 2(c). Within our expectations, the birefringence of the mixture is linearly proportional to the concentration of the terphenyl component, as Figure 2(a) shows. At 25°C, the birefringence of NLC-0100 mixture (100% terphenyls) reaches as high as 0.247. The NLC-6040 mixture shows $\Delta n=0.179$ while its melting point is below -50°C . This makes NLC-6040 an attractive candidate not only for research but also for commercial applications. To our surprise, the visco-elastic coefficient of these mixtures does not follow a linear behaviour as terphenyl concentration increases. We noticed that through the isothermote binary diagram of γ_1/K_{33} we can select a 'eutectic point-like composition' for visco-elastic coefficient, as shown in Figure 2(b). NLC-8020 and NLC-4060 have a lower visco-elastic coefficient than the host mixture (NLC-1000) and guest terphenyl mixture NLC-0100. This suggests that there might be a favourable molecular packing created between the rigid terphenyl molecules (Figure 3) and the cyclohexyl-biphenyl, bicyclohexyl-phenyl and

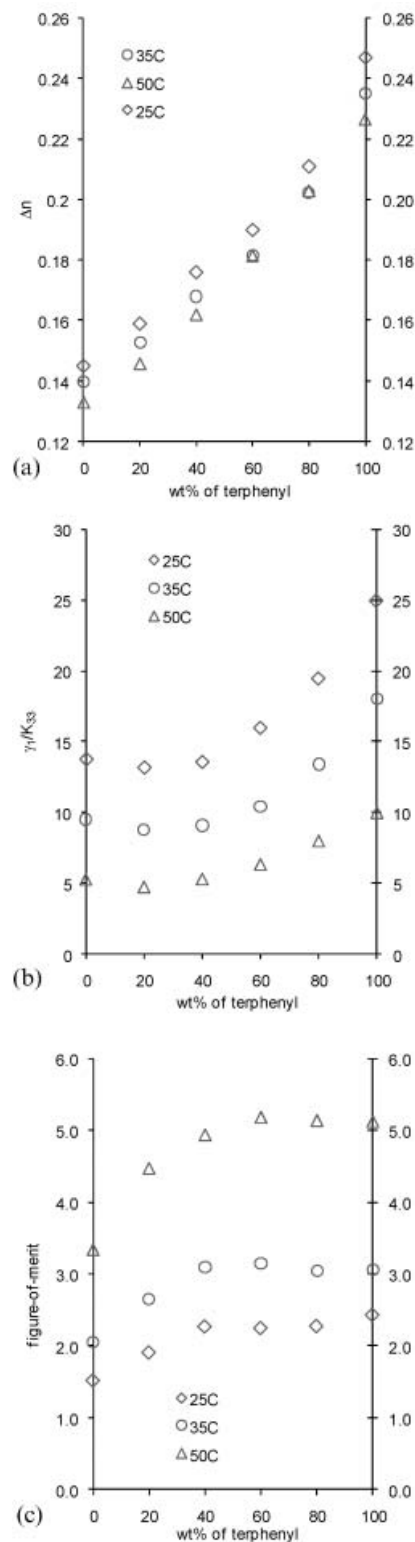


Figure 2. Isothermote diagrams of terphenyl concentration dependent (a) birefringence, (b) visco-elastic coefficient, and (c) figure-of-merit.

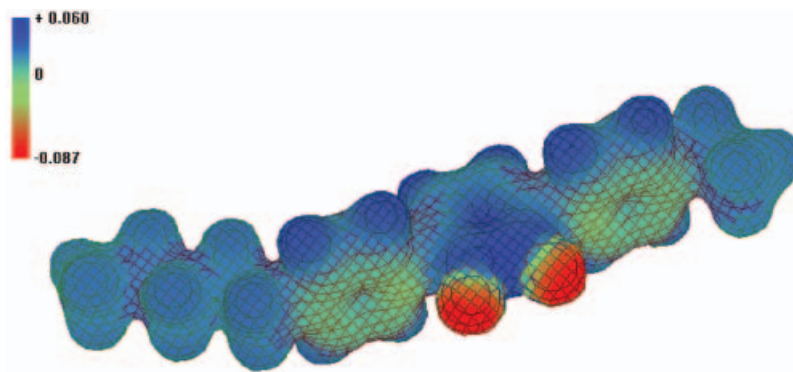


Figure 3. HyperChem simulated terphenyl molecule with isosurface of electrostatic potential shown. Geometry optimization by the MNDO method using the Polak–Ribiere algorithm.

cyclohexyl-phenyl molecules used in the host mixture. A negative charge introduced in the middle of the rigid core by two lateral fluorine atoms may produce disturbance in molecular spacing while not affecting alignment properties, which we will discuss later in this paper.

This surprising phenomenon is observed only when the terphenyl concentration does not exceed 50 wt% of the whole NLC formulation. Above this concentration, when terphenyl compounds become the majority, we observed that the visco-elastic coefficient increases as the terphenyl concentration increases, following typical additive behaviour. Consequently, the FoM follows a similar trend to γ_1/K_{33} and shows no additive effect with increasing terphenyl concentration (see Figure 2(c)). NLC-8020 and NLC-6040 show higher than the expected FoM due to their lower visco-elastic coefficient. When the terphenyl concentration exceeds 50 wt%, the FoM reaches a plateau. This is because the increased birefringence is compensated by the increased visco-elastic coefficient.

Among the NLC mixtures presented, NLC-6040 holds the best application potential. The 2',3'-difluoro-4-alkyl-4''alkyl-[1,1';4',1'']-terphenyl structure exhibits a relatively low visco-elastic coefficient; however, its dielectric anisotropy is also relatively small ($\Delta\epsilon \sim -2.5$ to -2.0), depending on the terminal chains (34, 39). To improve dielectric anisotropy, we introduced an asymmetrically fluorinated terphenyl structure 4-alkoxy-2,3-difluoro-4''alkyl-[1,1';4',1'']-terphenyl, which has been known for two decades (40, 41). This structure features a phenyl ring with an alkoxy terminal chain substituted laterally with two fluorine atoms, leading to $\Delta\epsilon \sim -5.4$ at standard experimental conditions. Therefore, NLC-6040 was further modified to NLC-6040M with 2,3-difluoro-4-alkoxy-4''alkyl-[1,1';4',1'']-terphenyl component in order to increase its dielectric anisotropy for lowering

the threshold and operating voltages. Doping an additional amount of terphenyl also increases the overall birefringence of the final composition. Detailed electro-optical performance results are depicted in Figure 4.

Figure 4(a) shows the birefringence measured within the entire temperature range of the nematic phase. In a LCoS projection display, the LC device is typically operated at 40 to 50°C because of the thermal effect of the arc lamp. Thus, as shown in Equation (5), it is desirable to employ a LC mixture which has a high clearing point so that the birefringence is not too sensitive to the temperature fluctuation. A high birefringence enables a thin cell gap to be used. This is a straightforward approach to shorten response time and reduce motion picture image blur.

NLC-6040M exhibits a ~ 140 to 150% increase in birefringence over the host mixture NLC-1000 within the temperature range of 20 to 50°C; however, their visco-elastic coefficients (Figure 4(b)) are quite similar. Therefore, NLC-6040M exhibits a much higher ($\sim 2 \times$) FoM (Figure 4(c)) than NLC-1000, regardless of the operating temperature chosen for LCoS. The FoM of NLC-6040M and NLC-1000 is $4.98 \mu\text{m}^2 \text{s}^{-1}$ and $2.23 \mu\text{m}^2 \text{s}^{-1}$ at 35°C and $\lambda = 633 \text{ nm}$. As mentioned above, we concentrated our effort on developing LC materials with high birefringence and high FoM because this will embed fast response time. A new mixture showing higher FoM will exhibit a shorter response time if the mixture is filled into an electro-optical cell with a properly adjusted cell gap.

Based on the measured data and Equations (2) and (4) we can compare the response time of a LCoS cell when filled with NLC-1000 or NLC6040M. Depending on the operating principles we assumed $d\Delta n = 320 \text{ nm}$ and $d\Delta n = 180 \text{ nm}$, respectively, for transmissive (T) mode and reflective (R) mode.

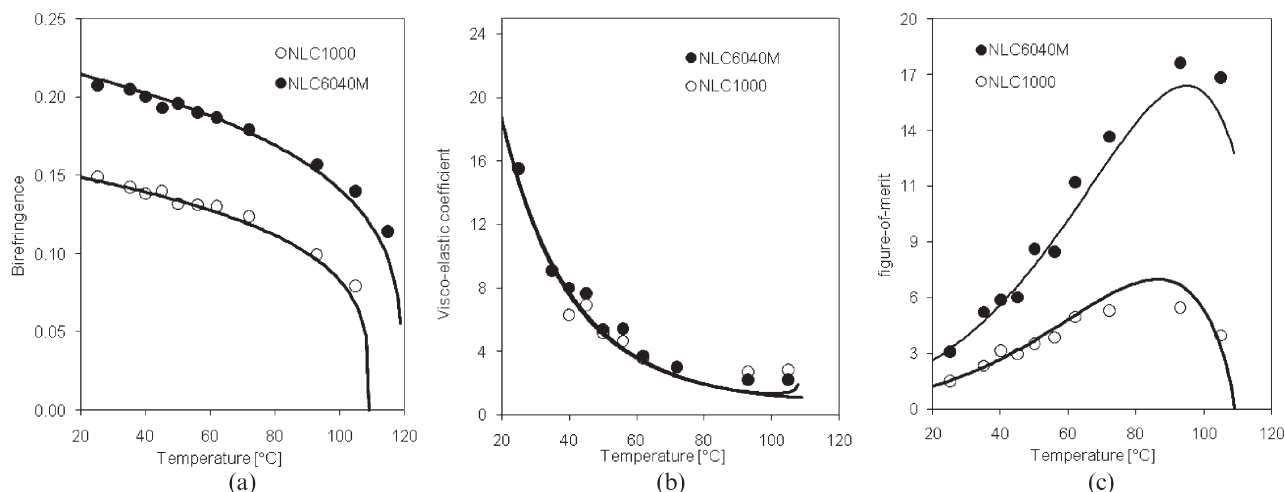


Figure 4. Temperature-dependent (a) birefringence, (b) visco-elastic coefficient, and (c) figure-of-merit of the host mixture NLC-1000 and its high-performance counterpart NLC-6040M.

Based on the birefringence of NLC-1000 mixture, the minimum cell gap for the T-mode was calculated to be 2.42, 2.53, and 2.73 μm , respectively, at 25, 35, and 50°C. Therefore, based on the elastic constant and rotational viscosity values, the calculated total response time was 8.2, 6.2, and 4.0 ms. Following similar procedures, the response time of NLC-6040M (with cell gap reduced to $\sim 1.7 \mu\text{m}$) was calculated to be 4.2, 2.8, and 1.6 ms, respectively, at 25, 35, and 50°C. This clearly shows that the response time of NLC-6040M is ~ 2 times faster than that of NLC-1000.

If we consider reflective mode operation, the obtained response time is 1.0, 0.7, and 0.4 ms for NLC-6040M versus 2.3, 1.5, and 1.0 ms for NLC-1000, respectively, at 25, 35, and 50°C. This is again a stunning 60 to 70% improvement over the NLC-1000 host mixture. These results clearly show the merit of increasing the birefringence by doping with terphenyl compounds.

In addition to birefringence and the FoM of the reported mixtures, we also measured their threshold voltage, dielectric and elastic properties; the results are listed in Table 2. The terphenyl modified mixture (NLC-6040M) exhibits a slightly decreased dielectric anisotropy which implies a slightly higher threshold voltage. This effect becomes important when the cell gap is reduced to around 1 μm (8). To enhance dielectric anisotropy of the presented material systems,

we could add some properly fluorinated biphenyl or terphenyl compounds (29, 39). As shown in Table 2, doping with terphenyl compound leads to a slight increase of a bend elastic constant K_{33} .

Alignment quality is an important issue during the course of developing VA LC devices. Previous studies show that it is more difficult to maintain good alignment in negative $\Delta\epsilon$ LC mixtures containing highly conjugated and rigid structures, especially at elevated temperatures (42, 43). Since our dopant compound is based on a terphenyl rigid core, we also evaluated the alignment quality of a filled VA cell. Figure 5 shows the voltage-dependent transmittance of two VA cells filled with NLC-1000 and NLC-6040M mixtures. The dark state of both cells is good. There is a noticeable difference in threshold voltage and phase retardation due to the difference in dielectric and optical anisotropies.

4. Conclusions

We have synthesised laterally fluorinated terphenyl LC compounds and evaluated their mesomorphic and electro-optic properties. Double lateral fluorination in the middle ring of 4-alkyl-4'-alkyl-[1,1';4',1'']-terphenyl structure was reported previously (29, 34) as having the least effect on rotational viscosity. Our experiment targeted developing a basic mixture formulation consisting of the homologues of

Table 2. Physical properties of NLC-1000, NLC-6040 and NLC-6040M mixtures.

LC MIX.	T_{MP} [°C]	T_C [°C]	V_{th}	$\epsilon_{ }$	ϵ_{\perp}	$\Delta\epsilon$	K_{11} [pN]	K_{22} [pN]	K_{33} [pN]
NLC-1000	< -50	109.4	2.44	3.45	7.22	-3.77	22.0	13.2	24.5
NLC-6040	< -50	110.1	2.96	3.42	6.46	-3.04	21.5	12.9	27.0
NLC-6040M	< -50	119.0	2.78	3.45	6.65	-3.20	24.4	15.2	27.4

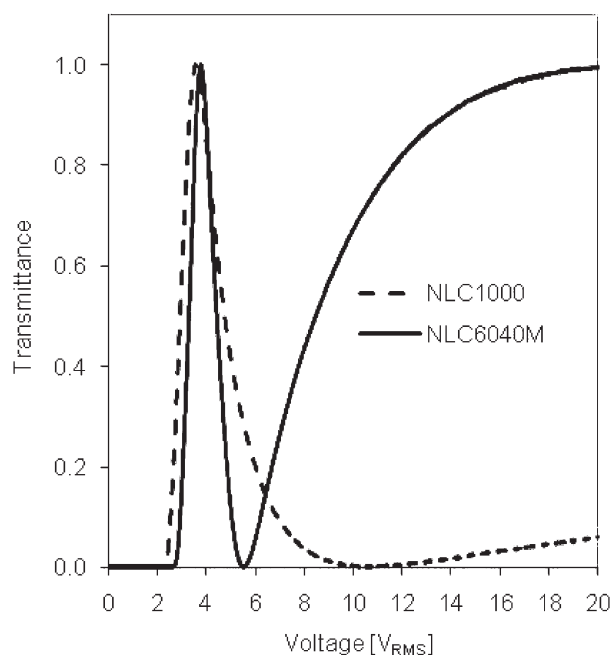


Figure 5. Voltage-dependent transmittance for NLC-1000 and NLC-6040M. Cell gap $d=8\mu\text{m}$, and $\lambda=633\text{ nm}$ at 23°C . Polarisers are crossed.

4-alkyl-4'-alkyl-[1,1';4',1'']-terphenyl structure and its further use as a dopant in high-birefringence and low-viscosity mixtures with negative dielectric anisotropy. The resultant mixture NLC0100 showed a dielectric anisotropy of -2.3 at room temperature. This result is in good agreement with Merck's data published in (29) for 2',3'-difluorosubstituted terphenyl single compound. In addition, proper formulation consisting of multiple homologues of 2',3'-difluorosubstituted terphenyl series resulted in a relatively wide nematic range of NLC0100 mixture. A two-bottle system NLC was evaluated with an increasing amount of fluorinated terphenyl component. Careful evaluation of each NLC mixture and proper formulation led us to the development of NLC-6040M mixture, whose FoM is about twice as high as that of the base NLC-1000 mixture. This is because the introduced NLC-0100 terphenyl mixture increases birefringence while keeping rotational viscosity more or less unchanged. The latter agrees well with Merck's data on the rotational viscosity of 2',3'-difluorosubstituted terphenyl compound (29). Moreover, the alignment quality and mesomorphic properties of NLC-6040M remain good. Applications of this mixture for LCoS projection displays and future LCD TVs are foreseeable.

References

- (1) Schiek M.F.; Fahrenschoen K. *Appl. Phys. Lett.* **1971**, *19*, 391–393.

- (2) Lyu J.J.; Sohn J.; Kim H.Y.; Lee S.H. *J. Disp. Technol.* **2007**, *3*, 404–412.
- (3) Armitage D.; Underwood I.; Wu S.T. *Introduction to Microdisplay*; Wiley: New York, 2006.
- (4) Ogata M.; Ukai K.; Kawai T. *J. Display Technol.* **2005**, *1*, 314–320.
- (5) Jakeman E.; Raynes E.P. *Phys. Lett.* **1972**, *39A*, 69–70.
- (6) Nehring J.; Kmetz A.R.; Scheffer T.J. *J. Appl. Phys.* **1976**, *47*, 850–857.
- (7) Nie X.; Lu R.; Xianyu H.; Wu T.X.; Wu S.T. *J. Appl. Phys.* **2007**, *101*, 103110-1–5.
- (8) Jiao M.; Ge Z.; Song Q.; Wu S.T. *Appl. Phys. Lett.* **2008**, *92*, 061102-1–3.
- (9) Gauza S.; Wang H.; Wen C.H.; Wu S.T.; Seed A.J.; Dąbrowski R. *Japan. J. Appl. Phys.* **2003**, *42*, 3463–3466.
- (10) Spadło A.; Dąbrowski R.; Filipowicz M.; Stolarz Z.; Przedmojski J.; Gauza S.; Fan Y.H.; Wu S.T. *Liq. Cryst.* **2003**, *30*, 191–198.
- (11) Gauza S.; Zhu X.; Wu S.T.; Piecek W.; Dąbrowski R. *J. Disp. Technol.* **2007**, *3*, 250–252.
- (12) Gauza S.; Wu S.T.; Spadło A.; Dąbrowski R. *J. Disp. Technol.* **2006**, *2*, 247–253.
- (13) Wu S.T.; Efron U. *Appl. Phys. Lett.* **1986**, *48*, 624–626.
- (14) Wang H.; Wu T.X.; Zhu X.; Wu S.T. *J. Appl. Phys.* **2004**, *95*, 5502–5508.
- (15) Gauza S.; Wen C.H.; Wu S.T.; Janarthanan N.; Hsu C.S. *Japan. J. Appl. Phys.* **2004**, *43*, 7634–7638.
- (16) Wu S.T.; Neubert M.; Keast S.S.; Abdallah D.G.; Lee S.N.; Walsh M.E.; Dorschner T.A. *Appl. Phys. Lett.* **2000**, *77*, 957–959.
- (17) Wu S.T.; Hsu C.S.; Shyu K.F. *Appl. Phys. Lett.* **1999**, *74*, 344–346.
- (18) Sekine C.; Konya N.; Minai M.; Fujisawa K. *Liq. Cryst.* **2001**, *28*, 1361–1367.
- (19) Wu S.T.; Cox R.J. *J. Appl. Phys.* **1988**, *64*, 821–826.
- (20) Seed A.J.; Toyne K.J.; Goodby J.W.; Hird M.J. *Mater. Chem.* **2000**, *10*, 2069–2080.
- (21) Sekine C.; Konya N.; Minai M.; Fujisawa K. *Liq. Cryst.* **2001**, *28*, 1495–1503.
- (22) Wu S.T.; Ramos E.; Finkenzeller U. *J. Appl. Phys.* **1990**, *68*, 78–85.
- (23) Wu S.T.; Margerum J.D.; Meng B.; Dalton L.R.; Hsu C.S.; Lung S.H. *Appl. Phys. Lett.* **1992**, *61*, 630–632.
- (24) Catanescu O.; Chien L.C. *Liq. Cryst.* **2006**, *33*, 115–120.
- (25) Goto Y.; Inukai T.; Fijita A.; Demus D. *Mol. Cryst. Liq. Cryst.* **1995**, *260*, 23–38.
- (26) Spells D.J.; Lindsey C.; Dalton L.R.; Wu S.T. *Liq. Cryst.* **2002**, *29*, 1529–1532.
- (27) Wu S.T.; Finkenzeller U.; Reiffenrath V. *J. Appl. Phys.* **1989**, *65*, 4372–4381.
- (28) Wand M.D.; Vohra R.T.; Thurmes W.N.; More K.M. *Ferroelectrics* **1996**, *180*, 333–339.
- (29) Pauluth D.; Tarumi K. *J. Mat. Chem.* **2004**, *14*, 1219–1227.
- (30) Geelhaar T.; Tarumi K.; Hirschmann H. *SID Tech. Digest* **1996**, *27*, 167–170.
- (31) Xianyu H.; Gauza S.; Song Q.; Wu S.T. *Liq. Cryst.* **2007**, *34*, 1473–1478.
- (32) Parish A.; Gauza S.; Wu S.T.; Dziaduszek J.; Dąbrowski R. *Liq. Cryst.* **2008**, *35*, 79–86.
- (33) Gauza S.; Parish A.; Wu S.T.; Spadło A.; Dąbrowski R. *Liq. Cryst.* **2008**, *35*, 483–488.
- (34) Pauluth D.; Tarumi K. *J. SID* **2005**, *13*, 693–702.
- (35) Wu S.T.; Efron U.; Hess L.D. *Appl. Opt.* **1984**, *23*, 3911–3915.

- (36) Wu S.T.; Lackner A.M.; Efron U. *Appl. Opt.* **1987**, *26*, 3441–3445.
- (37) Wu S.T.; Yang D.K. *Reflective Liquid Crystal Displays*; Wiley: New York, 2001.
- (38) Clark M.G.; Raynes E.P.; Smith R.A.; Tough R.J.A. *J. Phys. D: Appl. Phys.* **1980**, *13*, 2151–2164.
- (39) Gray G.W.; Hird M.; Lacey D.; Toyne K.J. *J. Chem. Soc. Perkin Trans.* **1989**, *2*, 2041–2053.
- (40) Kirsch P.; Reiffenrath V.; Bremer M. *Synlett* **1999**, *4*, 389–396.
- (41) Reiffenrath V.; Finkenzeller U.; Poetsch E.; Rieger B.; Coates D. *Proc. SPIE-Int. Soc. Opt. Eng.* **1990**, *1257*, 84–94.
- (42) Wen C.H.; Gauza S.; Wu S.T. *Appl. Phys. Lett.* **2005**, *87*, 191909–1–3.
- (43) Wen C.H.; Wu B.; Gauza S.; Wu S.T. *J. Displ. Technol.* **2005**, *2*, 234–239.